Green Synthesis of Silver Nanoparticles with Bioreductant from Lime Juice Powder (*Citrus aurantifolia*): Effect of Concentration and pH

Septian Dwi Mulyana, Retno Sari*, and Agus Syamsur Rijal

Department of Pharmaceutical Science, Faculty of Pharmacy, Universitas Airlangga, Surabaya 60115, Indonesia

* ***Corresponding author:***

email: retno-s@ff.unair.ac.id

Received: April 2, 2024
Accepted: May 8, 2024

DOI: 10.22146/ijc.95283

Abstract: *Significant development in antibacterial agents derived from metal nanoparticles is currently underway. One commonly employed type is silver nanoparticles (AgNPs), which display potential antibacterial activity at lower concentrations compared to other metals. Due to their high surface-to-volume ratio and small size, AgNPs can readily penetrate bacterial cell walls. Green synthesis methods of AgNPs, such as utilizing plants as reducing agents, offer substantial advantages over other synthesis techniques. Lime (*Citrus aurantifolia*), containing compounds like flavonoids and saponins, can serve as a natural reducing agent, converting Ag^+ ions to Ag^0. This study aims to evaluate the effects of $AgNO_3$ concentration, lime juice powder concentration, and pH on the formation and characteristics of AgNPs, as well as their activity against the bacteria* Propionibacterium acnes, Staphylococcus aureus, *and* Escherichia coli. *Results indicate that at an $AgNO_3$ concentration of 1 mM, lime juice extract at 1% with a pH of 9 produces optimal AgNP formation, with an absorbance of 4.631 and particle size of 68.4 nm. AgNPs exhibit higher antibacterial activity than $AgNO_3$. AgNPs synthesized with lime juice powder can increase their activity and have the advantages of being safe and environmentally friendly since they use plant material as a reducing agent.*

Keywords: *silver nanoparticles; green synthesis; lime juice powder; pH; antibacterial activity*

■ INTRODUCTION

In recent years, nanotechnology has garnered significant attention in the realm of future science and technology. Nano-sized materials (nanomaterials) offer distinct advantages such as large surface area and particle sizes ranging from 1–100 nm. Metal nanoparticles have emerged as a focus of research within this domain. Metals possess inherent antibacterial properties due to their ability to release metal ions that are toxic to bacteria [1]. Surface modification of metals is undertaken to enhance antibacterial activity and improve biocompatibility. The antimicrobial efficacy of metal nanoparticles stems from their nano-sized dimensions and extensive surface area, facilitating specific interactions with bacterial structures [2]. Various metals, including silver (Ag), gold (Au), zinc oxide (ZnO), copper (Cu), and iron (Fe), have been investigated for their antibacterial properties [3].

Silver nanoparticles (AgNPs) have garnered considerable attention due to their unique physicochemical properties compared to other materials, characterized by a high surface area-to-volume ratio, surface energy, and chemical reactivity [4]. With sizes ranging from 1–100 nm, AgNPs have demonstrated potential applications in cancer therapy, wound treatment, disinfection, and antibacterial agents [5]. Conventionally, AgNPs are synthesized through chemical or physical means, which involve hazardous substances and high temperatures or pressures, rendering them environmentally unfriendly and expensive. Consequently, there has been a shift towards green synthesis methods, using plants, algae, bacteria, and fungi for more economical, eco-friendly, and non-toxic AgNPs production [6].

Lime (*Citrus aurantifolia*) is a medicinal plant rich in bioactive compounds such as saponins, alkaloids,

tannins, phenolates, flavonoids, and terpenoids, exhibiting antioxidant, anti-inflammatory, antitumor, and antimicrobial activities [7]. The functional groups present in plant biomolecules can act as reducing agents in the conversion of Ag^+ ions to Ag^0 [8]. Lime has antimicrobial potential and is effective against both Gram-positive and Gram-negative bacteria, besides serving as an effective reducing and capping agent for AgNPs stability [9].

AgNPs size and shape have a role in their effectiveness as antibacterial agents. Smaller-sized AgNPs (< 100 nm) demonstrate superior antibacterial activity compared to larger nanoparticle sizes. Manipulating the AgNP synthesis parameters such as $AgNO_3$ concentration, extract quantity, pH, and incubation time allows control over nanoparticle characteristics [10-11]. $AgNO_3$ concentration significantly influences nanoparticle size and morphology. Higher $AgNO_3$ concentrations yield higher peaks of surface plasmon resonance (SPR) [11], indicating the rate of Ag^+ to AgNP conversion depends on $AgNO_3$ concentration. Moreover, $AgNO_3$ concentration directly impacts synthesis yield, with higher concentrations yielding greater yields [12-13]. AgNP synthesized using lime juice (*C. aurantifolia*) in liquid form with different incubation times showed the formation of AgNP at different wavelengths [9].

The concentration reductant significantly impacts the biosynthesis process and the properties of AgNPs, including their size and structure. A study by [14] observed that elevating the concentration of *Caulerpa serrulata* extract from 5 to 20% during AgNP synthesis amplifies the intensity of SPR and results in a shift towards a shorter wavelength (435 nm). This shift arises from the reduction in the average size of AgNPs. However, upon further escalation of the concentration to 25%, a decline in SPR intensity occurs owing to the aggregation of nanoparticles. This investigation demonstrates that aggregation occurs beyond a certain concentration threshold while augmenting the concentration can boost AgNPs production. Such aggregation can detrimentally affect functional properties. Consequently, for methods involving extracts, it is imperative to standardize the optimal concentration alongside other parameters [13].

As one of the crucial factors, pH influences the size and morphology of nanoparticles prepared through green synthesis. This is due to the electrical charge of biomass and capping agents undergoing significant alteration under varying pH conditions, leading to alterations in their capability to bind and reduce metal ions [15-16]. Several reports suggest that acidic environments yield larger-sized AgNPs, whereas smaller-sized AgNPs are formed in alkaline environments [17-18]. AgNPs synthesized using *Galega officinalis* extract in an alkaline pH environment result in smaller-sized AgNPs (10–20 nm) [19]. This study investigated the effect of $AgNO_3$ concentration, lime juice powder concentration and pH on AgNP formation. The AgNPs were evaluated for their particle size, polydispersity index, and antibacterial activity compared to $AgNO_3$.

■ EXPERIMENTAL SECTION

Materials

Materials in this study were silver nitrate ($AgNO_3$, Merck KgaA, Germany), sodium hydroxide (NaOH, Merck KgaA, Germany), and lime (*C. aurantifolia*) taken from Ujung Pangkah, Gresik, East Java, Indonesia and has been verified by expert botanist researchers from Materia Medika Indonesia, Batu, East Java, with document number 074/372/102.20-A/2022. Other materials, i.e., nutrient broth (Merck KgaA, Germany), nutrient agar (Merck KgaA, Germany), clindamycin hydrochloride (Xi'an Julong Bio-Tech Co., Ltd), *Propionibacterium acnes* (ATCC 11827) from BBLK Surabaya, *Staphylococcus aureus* (ATCC 6538), and *Escherichia coli* (ATCC 8739) were obtained from the Assessment Services Unit at Universitas Airlangga, Indonesia.

Instrumentation

Analytical balance (Ohaus PA-2102 C, USA), Fourier transform infrared (FTIR) spectrometer Bruker Eco-ATR (ALPHA II), magnetic stirrer (Thermo Scientific), UV-vis spectrophotometer (Hitachi UH5300), Delsa Nano C particle analyzer (Beckman Coulter), scanning electron microscope (SEM, Hitachi FlexSEM), micropipette, pH meter (SI Analytics Lab 865), drying oven binder ED 53 (Binder GmbH), freeze

dryer (Buchi, L-LyovaporTM L-200), and glasswares were used in this study.

Procedure

Sample preparation and freeze-drying of lime juice powder

Fresh limes were obtained from the Gresik area in East Java, Indonesia. The collected fruits were washed and halved to extract the juice manually. After obtaining the lime juice, it was filtered to obtain pure lime juice. Subsequently, the lime juice was frozen to produce lime juice powder using a freeze dryer. The freeze-drying process entailed freezing the lime juice at −40 °C, followed by vacuum drying for 3 weeks.

Synthesis of AgNPs with different concentrations of $AgNO_3$ and lime juice powder under various pH conditions (8, 9, 10)

The lime juice powder solution was prepared with concentrations of 1.00, 1.50, and 2.00%, while the $AgNO_3$ solution was prepared with concentrations of 0.50, 0.75, and 1.00 mM. A total of 25 mL of lime juice powder solution was added to 25 mL of $AgNO_3$ solution and stirred at 250 rpm for 1 h. The mixture of $AgNO_3$ solution and lime juice powder was then adjusted to the desired pH (pH 8–10) using 1 M NaOH and stirred at 250 rpm at room temperature for 1 h. Subsequently, the resulting mixture of AgNP solution was placed in an oven at 60 °C for 2 h, and color changes were observed. The influence of concentration and pH values was examined to compare the characteristics obtained.

Characterization of AgNPs

The synthesized AgNPs were characterized by assessing their absorbance using UV-vis spectroscopy across the wavelength range of 300–550 nm. Particle size and polydispersity Index (PDI) were determined using Delsa Nano C- Beckman Coulter. FTIR analysis was conducted to identify functional groups and ascertain the presence of any chemical interactions. The sample was appropriately positioned atop the attenuated total reflection (ATR) crystal. Subsequently, measurements were conducted within the wavenumber range of 400–4000 cm^{-1}. Particle morphology was examined using SEM. The sample was mounted on a carbon-coated holder, which was then inserted into a sputter coater for gold-palladium coating lasting approximately 120 s. Examination was carried out using an Inspect S50 type FP 2017/12 (Hitachi FlexSEM) at various magnifications, with measurements taken on multiple particles.

AgNP antibacterial activity testing

The antibacterial activity of AgNPs was conducted using standard test organisms: Gram-positive bacteria (*P. acnes*, *S. aureus*) and Gram-negative bacteria (*E. coli*). Bacterial suspensions were prepared by adding 0.9% NaCl solution and the turbidity of the bacterial suspension was determined using a UV-vis spectrophotometer at 580 nm until a %transmittance of 25–26 ± 1% was achieved.

To a 19.8 mL of sterile nutrient broth (NB) solution, 20 µL bacterial suspensions were added to attain a total volume of 20 mL. AgNP solutions were then added in volumes of 5, 10, 15, and 20 mL to NB solution and bacterial suspension. The mixture was then placed on an orbital shaker and incubated for 30 min. Further, 1 mL of the solution was extracted and added to 9 mL of fresh NB solution, which was then incubated at 37 °C for 24 h. Similar testing was conducted using an $AgNO_3$ solution. Clindamycin at a concentration of 50 ppm served as a positive control. The %transmittance of all treatments was assessed using a UV-vis spectrophotometer at 580 nm [20-21].

■ RESULTS AND DISCUSSION

Sample Preparation Lime Juice Powder

Lime juice powder from the freeze-drying process has a yellow color with a lime odor. Based on previous research that has carried out phytochemical screening using the thin-layer chromatography method, it is known that lime juice powder contains components such as flavonoids, saponins, terpenoids, steroids, and phenols [22].

Synthesis of AgNP with Different Concentrations of $AgNO_3$ and Lime Juice Powder at Various pH

The green synthesis of AgNP was conducted with variations in $AgNO_3$ concentrations, namely 0.50, 0.75, and 1.00 mM, and lime juice powder solution

concentrations of 1.0, 1.5, and 2.0% as a reductant, along with the influence of different pH values (8, 9, and 10), to determine the optimum conditions for AgNP formation, evaluated based on absorbance and particle size. The formation of AgNPs was characterized by a color change in the solution from clear to yellowish-brown (Fig. 1). The color change in the solution occurred due to the reduction of Ag^+ ions to Ag^0, resulting in the formation of AgNP [23]. Several factors play a role in forming AgNP, including the concentration of $AgNO_3$, concentration of the extract, reaction time, and pH, to accelerate the reaction rate. Additionally, secondary metabolites present in plants can function as natural bioreductants, thus contributing to nanoparticle formation by inducing the excitation of SPR in the particles [24-26]. Fig. 2 shows the mechanism of AgNP synthesis using biocompound from lime.

UV-vis spectrum analysis confirms the formation of AgNPs with a peak wavelength of 400 nm. The analysis results using a UV-vis spectrophotometer display the peak of the SPR. Typically, the SPR peak is influenced by the type of metal, particle size, shape, and morphology [27]. The absorbance measurement of AgNPs was conducted in the wavelength range of 300–550 nm. This is illustrated in Table 1, which presents the SPR peak and absorbance values for various concentrations of $AgNO_3$ and lime juice powder, notably strong at 400 nm. Values of λ_{max} below 400 nm indicate that the reduction process has not been completed, suggesting that the formed nanoparticles are Ag^+. The intensity of the SPR peak under basic pH conditions (8, 9, 10), reduced by lime juice powder, shifts towards shorter wavelengths and becomes narrower with increasing pH. This indicates a decrease in particle

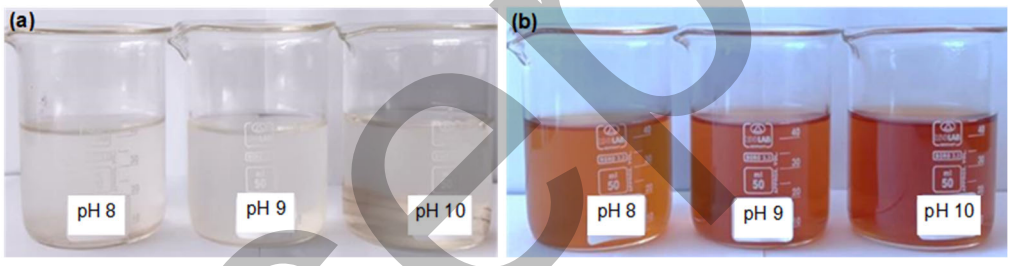

Fig 1. $AgNO_3$ solution and lime juice powder (a) before reaction and (b) after reaction

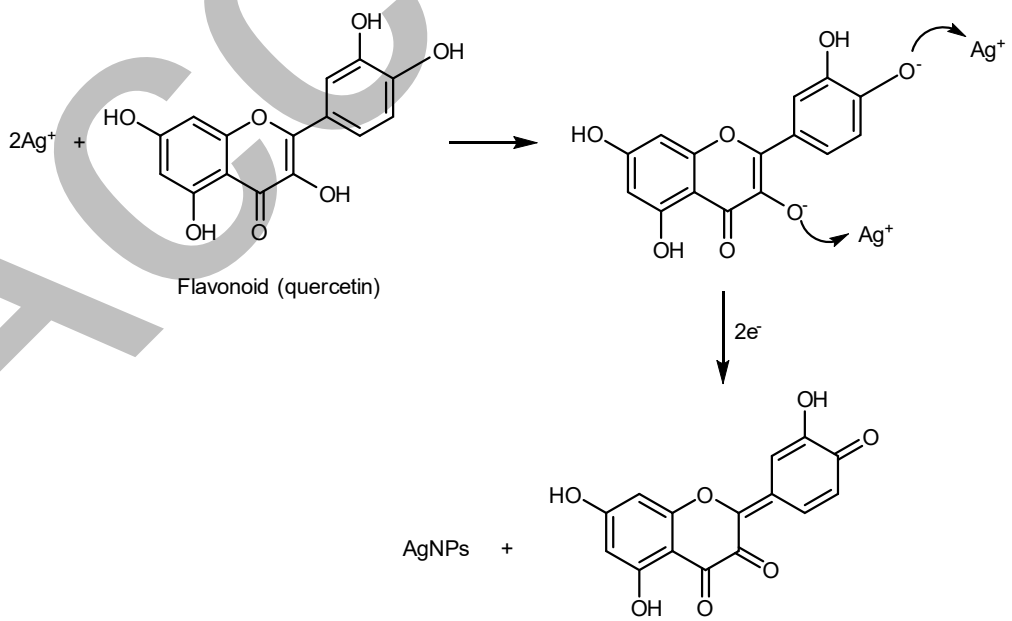

Fig 2. Illustration of the mechanism for the formation of AgNPs by green synthesis

Table 1. Absorbance value and particle size of AgNP synthesized with various $AgNO_3$ concentrations, lime juice powder concentrations and pH

Observation	Variable	Lime Juice Powder								
	$AgNO_3$	pH 8			pH 9			pH 10		
		1.0%	1.5%	2.0%	1.0%	1.5%	2.0%	1.0%	1.5%	2.0%
Particle size (nm)	0.50 mM	308.00	146.60	189.30	260.70	239.40	141.70	83.90	130.80	128.30
Absorbance		2.46	2.41	2.53	2.70	2.70	3.03	2.42	2.76	2.83
Particle size (nm)	0.75 mM	77.30	100.40	174.60	61.90	107.90	172.70	82.50	110.00	152.10
Absorbance		2.49	3.21	2.44	3.67	3.23	2.55	1.88	3.32	2.95
Particle size (nm)	1.00 mM	75.90	117.10	175.00	68.40	76.20	106.50	83.60	77.00	88.10
Absorbance		3.06	3.40	2.47	4.63	3.76	3.77	4.07	3.87	3.87

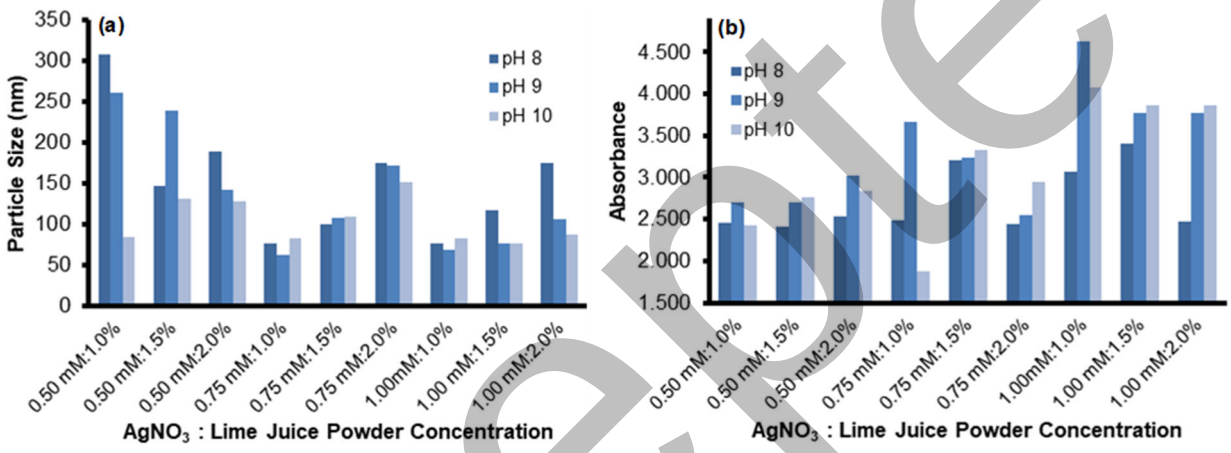

Fig 3. Histogram (a) particle size and (b) absorbance value of AgNP synthesized with various $AgNO_3$ concentrations, lime juice powder concentrations and pH

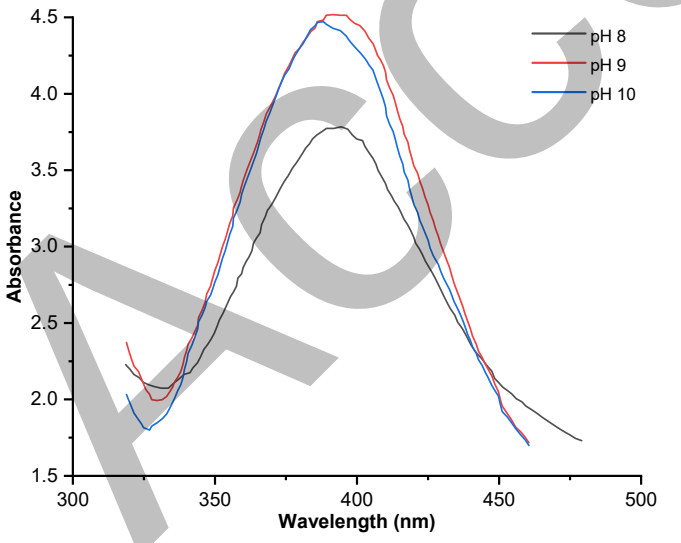

Fig 4. Spectra of AgNPs synthesized with 1 mM $AgNO_3$ and 1% lime juice powder at different pH

size and polydispersity of the nanoparticles [28]. Based on Table 1, Fig. 3 and Fig. 4, it can be observed that the absorbance peak of AgNPs falls within the range of 1.875–4.631. A low absorbance value indicates a small quantity of formed nanoparticles. However, the higher the absorbance value obtained, the greater the quantity of AgNP formed [29-35].

Increasing the concentration of lime juice powder as a reducing agent can expedite the formation rate of AgNPs. This acceleration is attributed to the heightened availability of biomolecules such as alkaloids, glycosides, flavonoids, saponins, and tannins, which serve as reductants, capping agents, and stabilizing agents, shielding the nanoparticles from aggregation [33,35]. Moreover, pH emerges as a pivotal factor influencing nanoparticle synthesis in this green synthesis method owing to its capability to modify the electric charge of biomolecules. This alteration may impact the capping ability, subsequently affecting nanoparticle stabilization and growth. Under low pH conditions, the SPR peak

tends to be diminished due to absorption by larger-sized nanoparticle forms [27]. Adjusting the pH during AgNP synthesis can be leveraged to govern specific characteristics such as nanoparticle morphology and size. Notably, at higher pH levels, there is heightened competition between protons and metal ions to establish bonds with negatively charged regions, leading to enhanced synthesis efficacy at alkaline pH [31]. It is apparent from Table 1 that the synthesis of AgNP with an $AgNO_3$ concentration of 1 mM and a lime juice powder concentration of 1% manifests an absorbance of 4.63 at pH 9 as seen in Fig 3 and 4.

Evaluation using the dynamic light scattering (DLS) method to obtain Z-average values (d.nm) and PDI constitutes a significant parameter in nanoparticle characterization [32]. The PDI value can gauge the degree of particle size distribution non-uniformity, stemming from the ratio of the average weight to the average molecular weight generated [34,36]. Furthermore, a PDI value approaching 0 denotes homogeneous particle size, while a PDI value < 0.3 signifies heterogeneous particle size [37]. Based on DLS measurements, the size of AgNP ranging from 61.9 to 308.0 nm on average was determined (Table 1). For AgNPs to traverse cell membranes and impede bacterial growth, the particle size should be smaller than 100 nm [38]. Various factors influence the formation of AgNP size, encompassing temperature, pH, $AgNO_3$ concentration, and reductant concentration, in achieving the desired size. The influence of $AgNO_3$ concentration can impact the size and morphology of synthesized nanoparticles. For example, in a study [11] employing $AgNO_3$ concentrations of 1–5 mM, it was noted that the higher the concentration, the larger the resulting size obtained. With increasing pH, the charge on biomolecules shifts from positive to negative, leading to robust repulsion between negatively charged $AgNO_3$ ions and biomolecules. The presence of larger nanoparticles at higher pH can be attributed to uncontrolled aggregation towards acidic pH owing to augmented $AgNO_3$ ion interactions. Conversely, heightened repulsion between ions with increasing pH may have hindered further nucleation, thus yielding smaller nanoparticles [11]. In comparison to AgNPs synthesized utilizing lime juice as a reductant [9], this study can yield considerably smaller particle sizes under basic conditions. Consequently, the findings suggest that escalating pH values can culminate in smaller particle sizes.

From the synthesis outcomes, it is discerned that a concentration of 1 mM $AgNO_3$ and 1% lime juice powder at pH 9 yields optimal results in AgNP synthesis. This is evidenced by a high absorbance value (4.631) and small particle size (68.400 nm) with a PDI of 0.251.

Spectroscopy ATR-FTIR Analysis

Spectroscopy ATR-FTIR analysis was undertaken to ascertain the functional groups of biomolecules engaged in reduction. The ATR-FTIR spectra of AgNPs are depicted in Fig. 5. The peak observed at the wavenumber of 3317 cm^{-1} indicates the presence of hydroxyl (–OH) groups and hydrogen bonding within the silver nanoparticles. Additionally, the peak at 2123 cm^{-1} suggests the involvement of stretching vibrations of symmetric and asymmetric C–H bonds from aliphatic –CH and $–CH_2$ groups in forming silver nanoparticles. Carbonyl groups are also discerned in the absorption band at the wavenumber of 1636 cm^{-1}. Compared with the ATR-FTIR spectra of lime juice powder, a minor shift from the wavenumber of 3389–3317 cm^{-1} is noted. This shift implies the potential role of amino groups, alkaloids, or terpenoids present in the

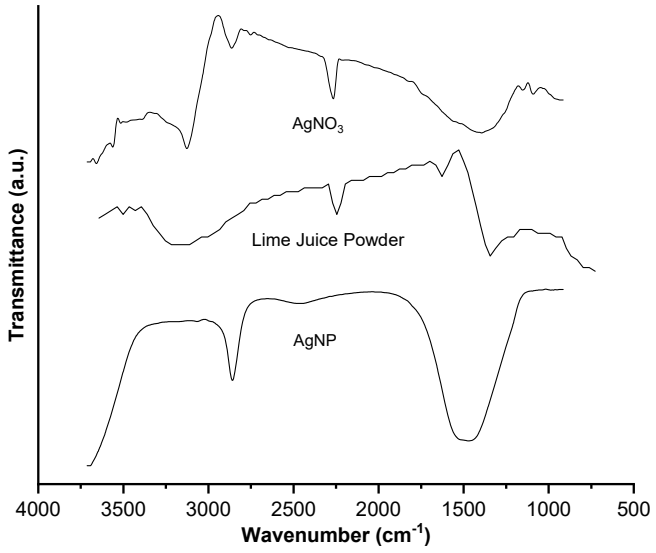

Fig 5. ATR spectra of AgNP formed from 1 mM $AgNO_3$ and 1% lime juice powder at pH 9

plant in the formation of AgNPs, functioning as reducing and stabilizing agents [9].

SEM Analysis

The results of the observations utilizing SEM with magnifications of 10,000× and 20,000× for AgNPs are depicted in Fig. 6. The morphology of AgNP at pH 9, as observed with SEM, reveals small spherical shapes that tend to aggregate, with particle sizes ranging between 50–100 nm (Fig. 6). Nanoparticles are prone to aggregation due to their high surface area, particularly when stored in liquid form. Various factors during synthesis are known to influence the physicochemical properties of AgNPs, leading to diverse actions and applications. The study conducted by Traiwatcharanon et al. [11] indicates that pH is a critical reaction parameter directly affecting size distribution, aggregation, particle morphology, and antimicrobial activity. As evidenced in the nanoparticle characterization in this study, pH variations result in AgNPs with distinct sizes and shapes [32].

AgNP Antibacterial Activity Test

The antibacterial activity of AgNPs was assessed to evaluate the impact of the formation and concentration of AgNPs on activity against Gram-positive (*P. acnes*, *S. aureus*) and Gram-negative (*E. coli*) bacteria. AgNP synthesized with 1 mM $AgNO_3$ and 1 lime juice powder at pH 9 has the smallest particle size and highest absorbance, which is used in this evaluation. Determination of AgNP antibacterial activity involved comparing %transmittance values of samples with the positive control. An antibiotic (clindamycin) was used as a positive control, while the negative control remained untreated. The results of the antibacterial activity test of AgNP are presented in Table 2 and Fig. 7.

Based on the results of the AgNP antibacterial activity test in Table 2 and Fig. 7, it can be seen that the %transmittance of AgNP is higher than $AgNO_3$ for *P. acnes*, *S. aureus*, and *E. coli*. Antibacterial activity is concentration-dependent. The bactericidal properties of AgNPs depend on their physicochemical properties, such as size, shape, particle surface charge, and characteristics of the bacterial species. Smaller particles are known to have more excellent antibacterial activity because they can easily reach the bacterial core, and their larger surface area leads to stronger interactions and

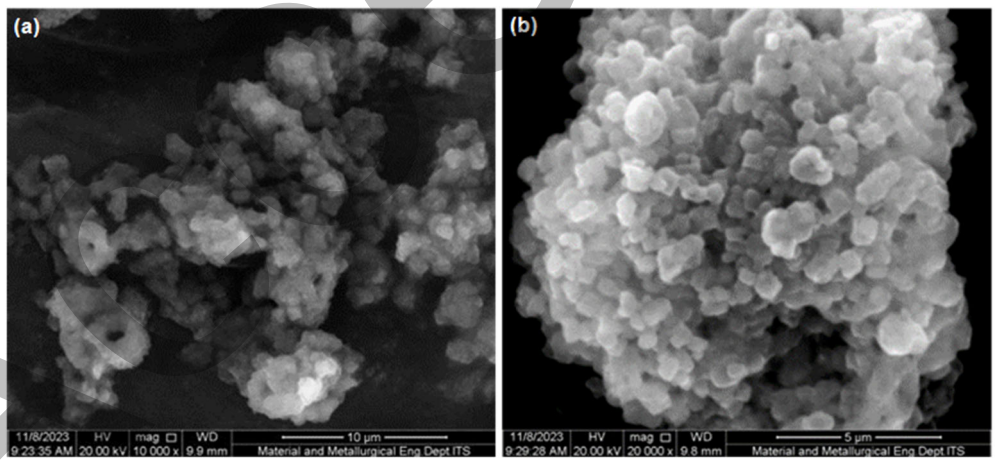

Fig 6. The SEM image of AgNPs with magnifications of (a) 10.000× and (b) 20.000×

Table 2. Antibacterial activity of AgNP, $AgNO_3$ against *P. acnes*, *S. aureus*, and *E. coli*

Bacteria	Control (+)	Control (−)	Transmittance (%)							
			$AgNO_3$ concentration (mM)				AgNP concentration (%)			
			0.125	0.250	0.375	0.500	0.125	0.250	0.375	0.500
P. acne	95.3	31.4	41.7	46.7	50.7	53.6	50.2	69.8	77.5	79.3
S. aureus	93.5	30.5	49.4	54.1	57.0	59.8	40.8	67.0	78.7	80.0
E. coli	89.6	28.4	35.5	37.3	40.1	43.6	38.6	44.8	59.1	74.0

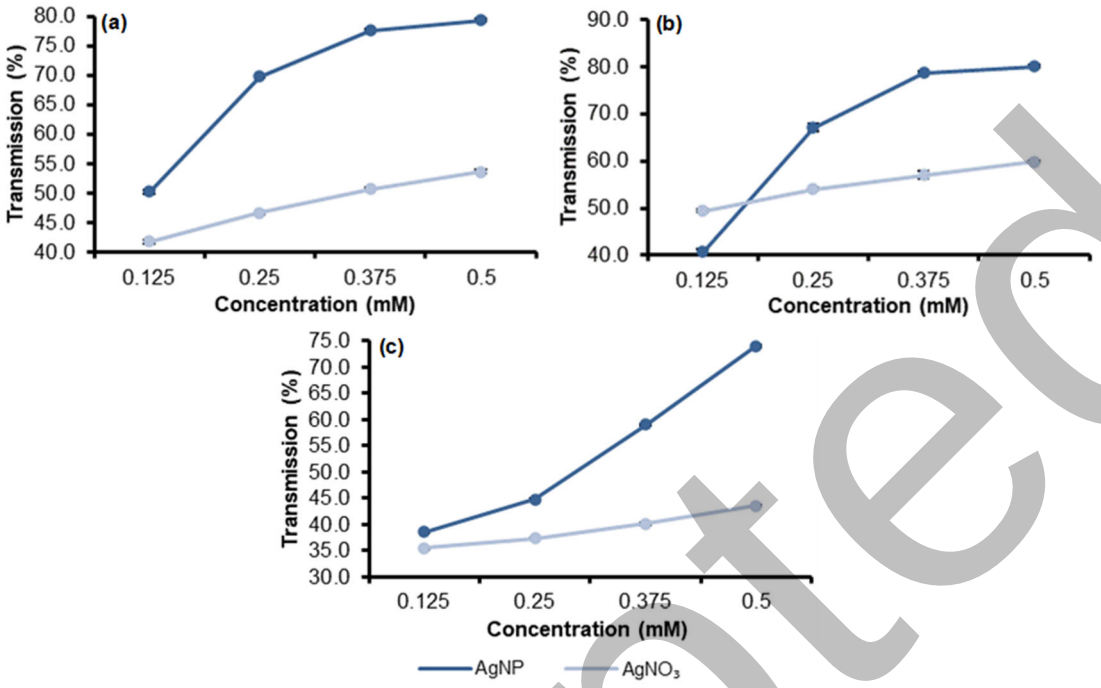

Fig 7. The result of the antibacterial activity test of AgNP against (a) *P. acnes*, (b) *S. aureus*, and (c) *E. coli*

bactericidal effects. Different forms may exhibit different antibacterial activities [39-40]. This effect may be related to differences in effective surface area and number of active sites. So, the antibacterial activity of AgNPs synthesized with lime juice powder is higher than $AgNO_3$ against *P. acnes*, *S. aureus*, and *E. coli*.

■ CONCLUSION

The concentration of $AgNO_3$ and lime juice extract as the reductant determines the synthesis outcomes of AgNPs, including absorbance values and particle size. Increasing the pH enhances the absorbance value and diminishes the particle size of AgNPs, with pH 9 being the optimal condition. AgNPs synthesized using 1 mM $AgNO_3$ and 1% lime juice powder at pH 9 exhibit a size of 68.4 nm. The antibacterial activity of AgNPs against *P. acnes*, *S. aureus*, and *E. coli* bacteria demonstrates higher growth inhibition compared to $AgNO_3$ solution and escalates with increasing AgNP concentration.

■ ACKNOWLEDGMENTS

The authors wish to acknowledge the Faculty of Pharmacy, Universitas Airlangga, Surabaya, Indonesia, for providing facilities.

■ CONFLICT OF INTEREST

The authors declared no conflict of interest.

■ AUTHOR CONTRIBUTIONS

Conceptualization, Septian Dwi Mulyana, Retno Sari, Agus Syamsur Rijal; Methodology, Septian Dwi Mulyana, Retno Sari; Software, Septian Dwi Mulyana; Validation, Retno Sari, Agus Syamsur Rijal; Formal Analysis, Septian Dwi Mulyana; Investigation, Septian Dwi Mulyana; Resources, Retno Sari, Agus Syamsur Rijal; Data Curation, Septian Dwi Mulyana; Writing - Original Draft, Septian Dwi Mulyana, Retno Sari; Writing - Review & Editing, Retno Sari, Agus Syamsur Rijal; Visualization, Septian Dwi Mulyana, Retno Sari, Agus Syamsur Rijal; Supervision, Retno Sari; Project Administration, Retno Sari; Funding Acquisition, Retno Sari.

■ REFERENCES

[1] Slavin, Y.N., Asnis, J., Häfeli, U.O., and Bach, H., 2017, Metal nanoparticles: Understanding the mechanisms behind antibacterial activity, *J. Nanobiotechnol.*, 15 (1), 65.

[2] Álvarez-Chimal, R., García-Pérez, V.I., Álvarez-Pérez, M.A., Tavera-Hernández, R., Reyes-Carmona, L., Martínez-Hernández, M., and Arenas-Alatorre, J.Á., 2022, Influence of the particle size on the antibacterial activity of green synthesized zinc oxide nanoparticles using *Dysphania ambrosioides* extract, supported by molecular docking analysis, *Arabian J. Chem.*, 15 (6), 103804.

[3] Jagadeeshan, S., and Parsanathan, R., 2019, "Nano-Metal Oxides for Antibacterial Activity" in *Advanced Nanostructured Materials for Environmental Remediation*, Eds. Naushad, M., Rajendran, S., Gracia, F., Springer International Publishing, Cham, Switzerland, 59–90.

[4] Ameen, F., Abdullah, M.M.S., Al-Homaidan, A.A., Al-Lohedan, H.A., Al-Ghanayem, A.A., and Almansob, A., 2020, Fabrication of silver nanoparticles employing the cyanobacterium *Spirulina platensis* and its bactericidal effect against opportunistic nosocomial pathogens of the respiratory tract, *J. Mol. Struct.*, 1217, 128392.

[5] Khan, Z.U.H., Khan, A., Chen, Y., Shah, N.S., Muhammad, N., Khan, A.U., Tahir, K., Khan, F.U., Murtaza, B., Ul Hassan, S., Qaisrani, S.A., and Wan, P., 2017, Biomedical applications of green synthesized Nobel metal nanoparticles, *J. Photochem. Photobiol., B*, 173, 150–164.

[6] Behravan, M., Hossein Panahi, A., Naghizadeh, A., Ziaee, M., Mahdavi, R., and Mirzapour, A., 2019, Facile green synthesis of silver nanoparticles using *Berberis vulgaris* leaf and root aqueous extract and its antibacterial activity, *Int. J. Biol. Macromol.*, 124, 148–154.

[7] Gupta, S., Rahman, M.A., and Sundaram, S., 2021, Citrus fruit as a potential source of phytochemical, antioxidant and pharmacological ingredients, *J. Sci. Healthcare Explor.*, 3 (1), 1–10.

[8] Borase, H.P., Salunke, B.K., Salunkhe, R.B., Patil, C.D., Hallsworth, J.E., Kim, B.S., and Patil, S.V., 2014, Plant extract: A promising biomatrix for eco-friendly, controlled synthesis of silver nanoparticles, *Appl. Biochem. Biotechnol.*, 173 (1), 1–29.

[9] Adebayo-Tayo, B.C., Akinsete, T.O., and Odeniyi, O.A., 2016, Phytochemical composition and comparative evaluation of antimicrobial activities of the juice extract of *Citrus aurantifolia* and its silver nanoparticles, *Niger. J. Pharm. Res*, 12 (1), 59–67.

[10] Pallela, P.N.V.K., Ummey, S., Ruddaraju, L.K., Pammi, S.V.N., and Yoon, S.G., 2018, Ultra small, mono dispersed green synthesized silver nanoparticles using aqueous extract of *Sida cordifolia* plant and investigation of antibacterial activity, *Microb. Pathog.*, 124, 63–69.

[11] Traiwatcharanon, P., Timsorn, K., and Wongchoosuk, C., 2017, Flexible room-temperature resistive humidity sensor based on silver nanoparticles, *Mater. Res. Express*, 4 (8), 085038.

[12] Rahman, A., Kumar, S., Bafana, A., Dahoumane, S.A., and Jeffryes, C., 2019, Biosynthetic conversion of Ag^{+} to highly stable Ag^{0} nanoparticles by wild type and cell wall deficient strains of *Chlamydomonas reinhardtii*, *Molecules*, 24 (1), 98.

[13] Chugh, D., Viswamalya, V.S., and Das, B., 2021, Green synthesis of silver nanoparticles with algae and the importance of capping agents in the process, *J. Genet. Eng. Biotechnol.*, 19 (1), 126.

[14] Aboelfetoh, E.F., El-Shenody, R.A., and Ghobara, M.M., 2017, Eco-friendly synthesis of silver nanoparticles using green algae (*Caulerpa serrulata*): Reaction optimization, catalytic and antibacterial activities, *Environ. Monit. Assess.*, 189 (7), 349.

[15] Rajkumar, R., Ezhumalai, G., and Gnanadesigan, M., 2021, A green approach for the synthesis of silver nanoparticles by *Chlorella vulgaris* and its application in photocatalytic dye degradation activity, *Environ. Technol. Innovation*, 21, 101282.

[16] Hamouda, R.A., Hussein, M.H., Abo-elmagd, R.A., and Bawazir, S.S., 2019, Synthesis and biological characterization of silver nanoparticles derived from the cyanobacterium *Oscillatoria limnetica*, *Sci. Rep.*, 9 (1), 13071.

[17] Siddiqui, M.N., Redhwi, H.H., Achilias, D.S., Kosmidou, E., Vakalopoulou, E., and Ioannidou, M.D., 2018, Green synthesis of silver nanoparticles and study of their antimicrobial properties, *J. Polym. Environ.*, 26 (2), 423–433.

[18] Hasan, M., Ullah, I., Zulfiqar, H., Naeem, K., Iqbal, A., Gul, H., Ashfaq, M., and Mahmood, N., 2018, Biological entities as chemical reactors for synthesis of nanomaterials: Progress, challenges and future perspective, *Mater. Today Chem.*, 8, 13–28.

[19] Manosalva, N., Tortella, G., Cristina Diez, M., Schalchli, H., Seabra, A.B., Durán, N., and Rubilar, O., 2019, Green synthesis of silver nanoparticles: Effect of synthesis reaction parameters on antimicrobial activity, *World J. Microbiol. Biotechnol.*, 35 (6), 88.

[20] Mohamed, N., and Madian, N.G., 2020, Evaluation of the mechanical, physical and antimicrobial properties of chitosan thin films doped with greenly synthesized silver nanoparticles, *Mater. Today Commun.*, 25, 101372.

[21] Augustine, R., Hasan, A., Yadu Nath, V.K., Thomas, J., Augustine, A., Kalarikkal, N., Al Moustafa, A.E., and Thomas, S., 2018, Electrospun polyvinyl alcohol membranes incorporated with green synthesized silver nanoparticles for wound dressing applications, *J. Mater. Sci.: Mater. Med.*, 29 (11), 163.

[22] Rahmiati, N., Sari, R., and Wahyuni, T.S., 2023, Phytochemical and antioxidant activity evaluation of lime (*Citrus aurantifolia*) juice powder, *J. Farm. Galenika*, 9 (2), 197–207.

[23] Chowdhury, R.A., Dhar, S.A., Das, S., Nahian, M.K., and Qadir, M.R., 2021, Green synthesis and characterization of silver nanoparticles from the aqueous extract of the leaves of *Citrus aurantifolia*, *Mater. Today: Proc.*, 44, 1039–1042.

[24] Siddiqi, K.S., Husen, A., and Rao, R.A.K., 2018, A review on biosynthesis of silver nanoparticles and their biocidal properties, *J. Nanobiotechnol.*, 16 (1), 14.

[25] Marslin, G., Siram, K., Maqbool, Q., Selvakesavan, R.K., Kruszka, D., Kachlicki, P., and Franklin, G., 2018, Secondary metabolites in the green synthesis of metallic nanoparticles, *Materials*, 11 (6), 940.

[26] Dada, A.O., Adekola, F.A., Dada, F.E., Adelani-Akande, A.T., Bello, M.O., Okonkwo, C.R., Inyinbor, A.A., Oluyori, A.P., Olayanju, A., Ajanaku, K.O., and Adetunji, C.O., 2019, Silver nanoparticle synthesis by *Acalypha wilkesiana* extract: Phytochemical screening, characterization, influence of operational parameters, and preliminary antibacterial testing, *Heliyon*, 5 (10), e02517.

[27] Priya, R.S., Geetha, D., and Ramesh, P.S., 2016, Antioxidant activity of chemically synthesized AgNPs and biosynthesized *Pongamia pinnata* leaf extract mediated AgNPs – A comparative study, *Ecotoxicol. Environ. Saf.*, 134 (Part 2), 308–318.

[28] Marciniak, L., Nowak, M., Trojanowska, A., Tylkowski, B., and Jastrzab, R., 2020, The effect of pH on the size of silver nanoparticles obtained in the reduction reaction with citric and malic acids, *Materials*, 13 (23), 5444.

[29] Gunsolus, I.L., Mousavi, M.P.S., Hussein, K., Bühlmann, P., and Haynes, C.L., 2015, Effects of humic and fulvic acids on silver nanoparticle stability, dissolution, and toxicity, *Environ. Sci. Technol.*, 49 (13), 8078–8086.

[30] Maarebia, R.Z., Wahab, A.W., and Taba, P., 2019, Synthesis and characterization of silver nanoparticles using water extract of sarang semut (*Myrmecodia pendans*) for blood glucose sensors, *Indones. Chim. Acta*, 12 (1), 29–46.

[31] Sintubin, L., De Windt, W., Dick, J., Mast, J., van der Ha, D., Verstraete, W., and Boon, N., 2009, Lactic acid bacteria as reducing and capping agent for the fast and efficient production of silver nanoparticles, *Appl. Microbiol. Biotechnol.*, 84 (4), 741–749.

[32] Miranda, A., Akpobolokemi, T., Chung, E., Ren, G., and Raimi-Abraham, B.T., 2022, pH alteration in plant-mediated green synthesis and its resultant impact on antimicrobial properties of silver nanoparticles (AgNPs), *Antibiotics*, 11 (11), 1592.

[33] Alafandi, L., Nasaruddin, R.R., Aziz, A.H.A., Engliman, N.S., and Mastuli, M.S., 2021, Green synthesis of silver nanoparticles using coffee extract for catalysis, *MNIJ*, 1 (2), 13–25.

[34] Kane, S.N., Mishra, A., and Dutta, A.K., 2016, Preface: International conference on recent trends in physics (ICRTP 2016), *J. Phys.: Conf. Ser.*, 755 (1), 011001.

[35] Chadha, R., Maiti, N., and Kapoor, S., 2014, Reduction and aggregation of silver ions in aqueous citrate solutions, *Mater. Sci. Eng., C*, 38, 192–196.

[36] Badmus, J.A., Oyemomi, S.A., Adedosu, O.T., Yekeen, T.A., Azeez, M.A., Adebayo, E.A., Lateef, A., Badeggi, U.M., Botha, S., Hussein, A.A., and Marnewick, J.L., 2020, Photo-assisted bio-fabrication of silver nanoparticles using *Annona muricata* leaf extract: Exploring the antioxidant, anti-diabetic, antimicrobial, and cytotoxic activities, *Heliyon*, 6 (11), e05413.

[37] Handayani, W., Ningrum, A.S., and Imawan, C., 2020, The role of pH in synthesis silver nanoparticles using *Pometia pinnata* (Matoa) leaves extract as bioreductor, *J. Phys.: Conf. Ser.*, 1428 (1), 012021.

[38] Franco, D., Calabrese, G., Guglielmino, S.P.P., and Conoci, S., 2022, Metal-based nanoparticles: Antibacterial mechanisms and biomedical application, *Microorganisms*, 10 (9), 1778.

[39] Mishra, A., Pradhan, D., Halder, J., Biswasroy, P., Rai, V.K., Dubey, D., Kar, B., Ghosh, G., and Rath, G., 2022, Metal nanoparticles against multi-drug-resistance bacteria, *J. Inorg. Biochem.*, 237, 111938.

[40] Kumari, S.C., Dhand, V., and Padma, P.N., 2021, "Green Synthesis of Metallic Nanoparticles: A Review" in *Nanomaterials: Application in Biofuels and Bioenergy Production Systems*, Eds. Kumar, R.P., and Bharathiraja, B., Academic Press, Cambridge, MA, US, 259–281.